Electrochemical corrosion behaviour of dental alloys and metals in artificial saliva

P. Battaini

Different rehabilitation solutions are very often adopted for the same oral cavity. Unfortunately, the combination of different metallic materials may cause galvanic corrosion. This work is aimed at the electrochemical characterization of some dental materials in artificial saliva. Precious metals alloys as well as titanium, dental amalgam and a Co-Cr alloy are considered. The results show that all alloys and titanium are characterized by low corrosion currents and negligible galvanic corrosion. On the contrary, significant galvanic corrosion currents are measured in couplings with the dental amalgam.

1. INTRODUCTION

Lots of diversified and complex solutions exist for dental prosthesis rehabilitation. The replacement of a single tooth and the realization of removable or fixed bridges for partial or complete prostheses, are carried out by the use of different materials. Also, the preservation of a single tooth is accomplished by the application of various techniques that may require amalgams or metal alloys. Frequently, combinations of materials such as amalgams, precious metals alloys, titanium, cobalt-chromium alloys etc. are adopted in the same oral cavity (1,2).
Recently, the use of Ti in removable prosthodontics (3) increased remarkably. In the last 20 years, titanium played an important role as implant material, for the substitution of single tooth or complete prostheses (4,5). These implants are a portion of the prosthesis and provide the proper anchoring to the mandibular bone. The prosthesis is finished with precious metal alloys superstructures, which are - in turn - provided with esthetical ceramic coating.
As a consequence, different interfaces develop between materials and environment. The latter may be the mandibular bone, a metal alloy, the oral cavity with all its complex fluids, ceramic materials or plastic resins, or a combination of that. In case of alloys an electrochemical process of corrosion may develop, thanks to the different body fluids. On a corroding alloy or metal, anode and cathode sites exist. In case of two alloys electrically in contact, the more noble alloy reduces its corrosion rate and its anodic reaction rate is suppressed. Conversely, the less noble alloy increases its corrosion rate and its cathodic reaction rate is suppressed. This process of galvanic corrosion is represented by the following simultaneous reactions:

• Cathodic reactions:

$O_2 + 4e^- + 2H_2O = 4OH^-$

$O_2 + 4H^+ + 4e^- = 2H_2O$

• Anodic reaction:

$Me = Me^{n+} + ne^-$

The in vitro study of the galvanic process is very difficult, because its intensity depends on many parameters, like the pH, the composition and conductivity of the electrolytic medium, its aeration or de-aeration, the electrode potential, and the surface ratio between the anode and the cathode.
Frequently, oxygen is in contact with the material surface exposed to the fluids of the oral cavity. Free metal surfaces occur in amalgam reconstruction, titanium frameworks, and alloy-ceramic or alloy-resin reconstruction. In vivo corrosion phenomena are well documented in these cases. Very often, they are observed at brazed joints or defects like porosity, inclusions etc.
A lot of works showed the criticality of galvanic corrosion combined with crack corrosion. This coupling is significant for pH reduction and increase of Cl^- ion concentration simultaneous to local reduction of dissolved oxygen concentration (6,7,8,9).
This work is aimed to characterize the corrosion of dental alloys, amalgams and commercially pure metals (Ti, Pd, Au) in artificial saliva in oxygen environment, by electrochemical techniques.

2. MATERIALS AND METHODS

2.1. Specimen preparation

Dental alloys, amalgam and pure metals were considered in this work. Their chemical composition is reported in Table 1. The dental alloys were cast by the lost wax process, as discs of 15 mm diameter and 3 mm thickness. Each disc was subjected to a homogenize treatment at 950°C for 10 minutes followed by air-cooling.
The amalgam specimen was obtained by manual condensation according to the producer instructions and applying the same methods used for condensation in the oral cavity. This specimen was obtained as a disc with the above cited dimensions, 5 years before testing. In fact, it is known that ageing makes the amalgam more appropriate for the evaluation of long-term behaviour, since the release of metallic ions decreases in time (10). The amalgam is a non-gamma 2-type.
Alloy and amalgam specimens were previously polished for microstructural investigation.
Before electrochemical testing, the specimen surface was subjected to dry grinding by 600-grit SiC sheet. Residuals from grinding were removed from the surface by dehumidified and purified air jet.
Discs with the above mentioned shape and dimensions were obtained by mechanical tooling from commercial ingots of the three pure metals, Au, Pd and Ti.

P. Battaini, *8853 spa, Legnano*

Memoria pervenuta a febbraio 2000

Alloy	Au	Pt	Pd	Ag	Cu	In	Sn	Ga	Zn	Co	Cr	Mo	W	Hg	Ti
A	2.0		74.7		9.4	6.5		4.9	2.2						
B	6.0		74.8	6.5		6.5		5.9							
C			61.3	24.5		2.1	10.0		1.0						
D			56.1	33.5			7.8	2.5							
E	43.0		30.8	19.8			5.9								
F	51.5		38.4			8.5									
G	88.7	9.46													
H										61.0	25.3	7.0	5.0		
Amalg.				26.0	4.4		12.8		0.7					56.0	
Au	99.99														
Pd			99.95												
Ti															99.0

Table 1. Chemical composition of alloys metals and amalgam (weight %).

Tab.1. Composizione chimica di leghe, metalli e amalgama (%in peso).

	Scan rate (mV/s)	V initial (mV)	V final (mV)
Potentiodynamic polarization	0.166	-200 vs. OCP	+ 900 vs. SCE
Polarization Resistance	0.1	-20 vs. OCP	+ 20 vs. OCP
Tafel	0.1	0 vs. OCP	± 250 vs. OCP
Ecorr	--	- 1250 vs. SCE	--

Table 2. Operating conditions used in the electrochemical tests.

Tab.2. Condizioni operative usate nelle prove elettrochimiche.

2.2. Microstructural investigation

Microstructural investigation was performed by Scanning Electron Microscopy (SEM). In order to get a morphological and chemical characterization of phases and structural constituents, the polished specimens were analysed in the backscattered electrons mode and by energy dispersive spectrometry.

2.3. Electrochemical measurements

The electrochemical behaviour was studied in Ringer-type artificial saliva with the following chemical composition: NaCl 9 g/l; KCl 0.4 g/l; $NaHCO_3$ 0.2 g/l; $CaCl_2 6H_2O$ 0.25 g/l.

The solution was maintained stagnant at 37 °C. Measurements were performed by means of a 3-electrodes electrochemical cell, equipped with a saturated calomel electrode (SCE) as reference and a platinum electrode. Each specimen was mounted and sealed by PTFE, and provided with a working surface of 1 cm^2. Measurement monitoring was performed by an EG&G PAR mod. 273A potentiostat/galvanostat. Potentiodynamic curves, Tafel curves (11) and curves for polarization resistance (R_p) calculation were obtained.

Four anodic and four cathodic Tafel curves and four curves for R_p determination were obtained from each specimen. These measurements were performed in order to calculate the corrosion rate I_{corr} according to the Stearn & Cjlary equation. The open circuit potentials were measured by two different methodologies. In the first case, they were measured after immersion in Ringer solution until a variation less than 0.01 mV/s was attained and were called OCP. In the second case, they were measured after immersion in Ringer solution until a variation less than 0.01 mV/s and a subsequent cathodic polarization at -1250 mV vs SCE for 300 s were attained and were called E_{corr}. The E_{corr} values were recorded during the following 36 hours. Table 2 summarizes the operating conditions.

2.4. Galvanic corrosion

Tests were performed in stagnant Ringer solution at 25 °C in a cell with the working electrodes mounted horizontally and opposed each other. Each electrode was mounted and sealed by PTFE, with a ratio between anodic and cathodic surfaces equal to 1. The current was monitored as a function of time by an EG&G PAR mod. 273A potentiostat/galvanostat modified as a zero resistance ammeter according to the producer's instructions. With this modification, measurements of current variations up to 100 pA and simultaneous evaluation of galvanic current and couple potential (E couple) can be performed.

3. RESULTS AND DISCUSSION

3.1. Microstructural investigation

All alloys could be well investigated by SEM in the backscattered electrons mode. Micrographies are shown in Figs. 1 to 4. From this investigation alloys C and G - not shown in the figures – turn out to be homogeneus, while alloy B shows some inhomogeneity (see fig.1). The inhomogeneous microstructure in precious metal alloys is due to the preferential concentration of low atomic number and low corrosion resistance elements (Cu, In, Sn) in some phases. As a consequence, a higher propensity to corrosion should be expected in the less homogeneous alloys (12, 13), due to the formation of anodic zones at poorly noble phases.

3.2. Electrochemical measurements

The potentiodynamic curves (Figs. 5, 6, 7 and 8) give the critical passivation current (I_{crit}), which describes the passivation capability of the metal or alloy. While the dental amalgam shows a low passivation susceptibility (fig. 5), the other alloys and pure metals are characterized by $I_{crit} < 3500$ nA/cm^2. Particularly, the Ti passivation tendency is similar to that of alloy C and higher than that of alloy D (see Figs. 5, 8). The potentiodynamic curves differ significantly. As shown in Figs. 5 to 7, the high gold content alloys (G, E), the Au-Pd alloy (F) and the pure metals Ti, Au and Pd exhibit a wide range of low current density (10^{-9} to 10^{-5}) between the corrosion potential [E(I=0)] and the breakdown potential. This behaviour is typical of high corrosion resistance materials. Particularly, alloy E undergoes the highest current density variation between the above mentioned potentials (Fig. 6). High Pd content alloys (A and B) are characterized by secondary passivation at a potential of about 700mV vs SCE (Fig. 7), which is not observed in pure Pd. Even if alloy A is less homogeneous in microstructure than B, the latter shows a hi-

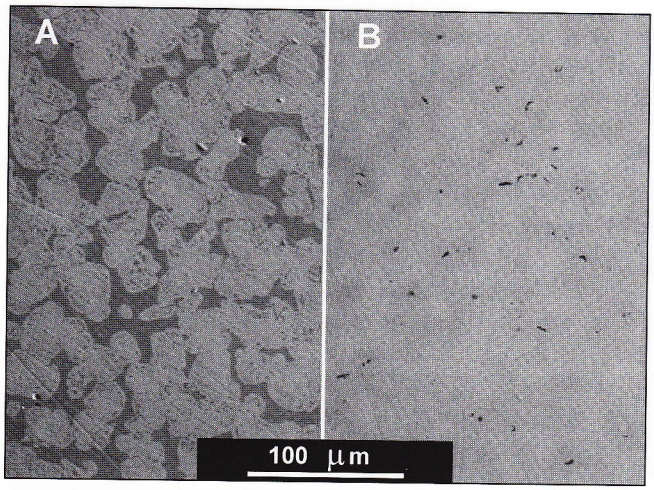

Figure 1. Backscattered electrons SEM image.
Left: Microstructure of high Pd content alloy A. The dark phase is mainly composed by In, Cu and Ga.
Right: Microstructure of high Pd content alloy B. The small dark phases with dimension less than 10 µm are In-Ga isles.

Figura 1. Immagine SEM ad elettroni retrodiffusi.
Sinistra: Microstruttura della lega A ad alto titolo di Pd. La fase scura è composta principalmente da In, Cu e Ga.
Destra: Microstruttura della lega B ad alto titolo di Pd. Le piccole fasi scure con dimensioni inferiori ai 10 µm sono composte da In e Ga.

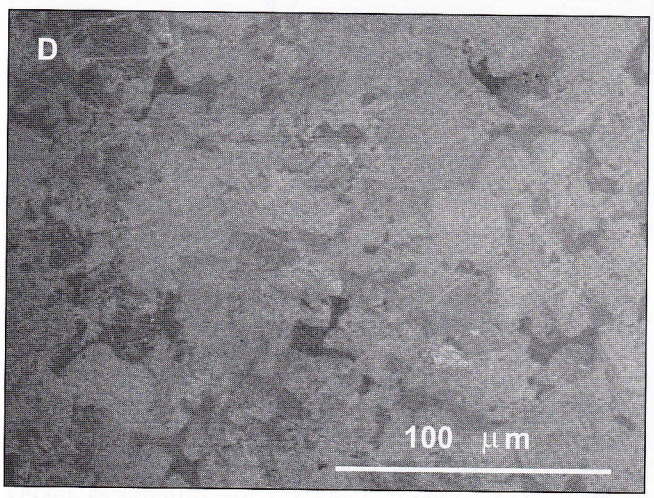

Figure 2. Backscattered electrons SEM image showing the microstructure of the Pd-Ag alloy D. An inhomogeneous distribution of Sn and Ga concentrating in the darker regions is visible.

Figura 2. Immagine SEM ad elettroni retrodiffusi. Microstruttura della lega D al Pd-Ag. Distribuzione disomogenea di Sn e Ga che si concentrano nelle zone più scure.

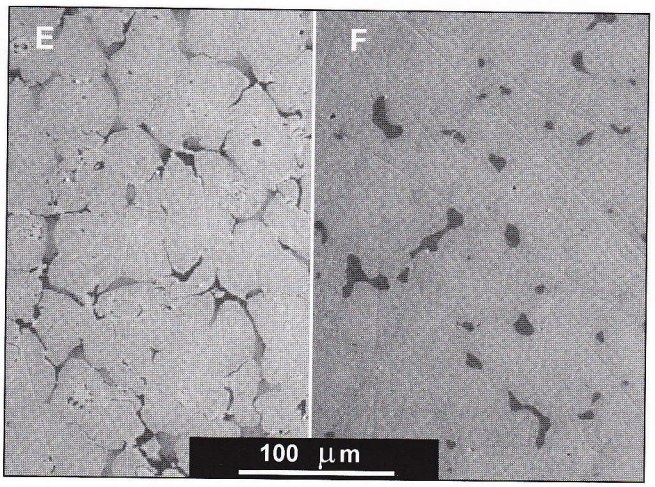

Figure 3. Backscattered electrons SEM image.
Left: microstructure of the Au-Pd-Ag alloy E. The grain boundary precipitation of a high Sn content phase is revealed.
Right: Microstructure of the Pd-Au alloy F. High In content isles are present.

Figura 3. Immagine SEM ad elettroni retrodiffusi.
Sinistra: Microstruttura della lega E con Au-Pd-Ag : presenza di una fase ad elevato contenuto di Sn che decora i bordi di grano.
Destra: Lega F al Pd-Au: isole ad alto contenuto di In.

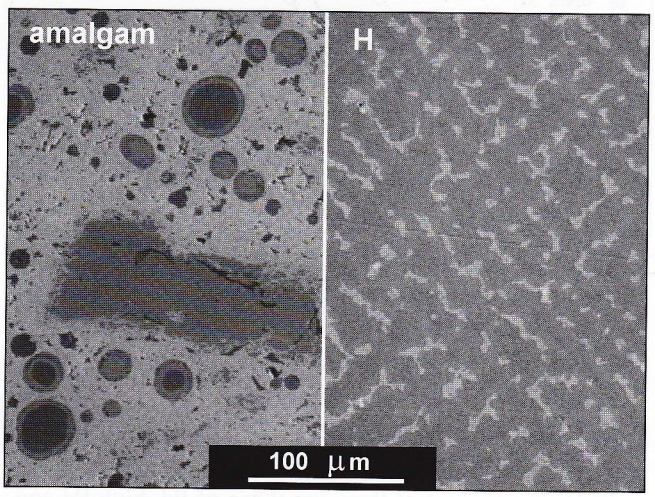

Figure 4. Backscattered electrons SEM image.
Left: Microstructure of the non-gamma 2-type dental amalgam. The matrix is Ag_2Hg_3. It includes phases composed by Ag, Cu and Sn.
Right: Co-Cr alloy H. A dendritic microstructure and Mo-rich phases (bright in the image) are revealed.

Figura 4. Immagine SEM ad elettroni retrodiffusi.
Sinistra: Amalgama dentale del tipo non-gamma 2. Matrice del tipo Ag_2Hg_3 con varie fasi contenenti Ag, Cu, Sn al suo interno.
Destra: Lega H al Co-Cr con struttura dendritica e fasi ricche in Mo (chiare nell'immagine).

gher I_{crit} than the former and a more remarkable peak at 700 mV. Anyway, these three materials have similar corrosion potentials [E(I=0)] and their current density is less than 5 x 10^{-6} A/cm^2 before the transpassive region (Fig. 7).
The Pd-Ag alloys (C and D) undergo a passivation process with a primary passivation potential of about 400 mV vs SCE (Fig. 8). They are not characterized by secondary passivation at 700 mV vs SCE, typical of high Pd content alloys. They have a corrosion potential [E(I=0)] lower than pure Pd, the smallest value being that of the alloy with the highest Ag content. The passive current density of these alloys lies between 5 x 10^{-6} and 0.8 x 10^{-7} A/cm^2, similarly to high Pd content alloys. The alloy with the most inhomogeneous microstructure (D) has the lowest corrosion potential [E(I=0)] and the highest passive current density.
The amalgam passive region is very narrow, ranging from -300 and -200 mV vs SCE, while the passive current is high (10^{-4} A/cm^2), showing a clear propensity to corrosion at high voltage (Fig. 5).
Alloy H (Co-Cr) has a passive region limited between 0 and 200 mV vs SCE. However, it shows corrosion currents lower than 10^{-5} A/cm^2 for potentials up to +500 mV vs SCE (Fig. 5).
The OCP values of Ti, alloy H and amalgam (Tables 3 and 4) lie between -200 and -300 mV vs SCE while those of the

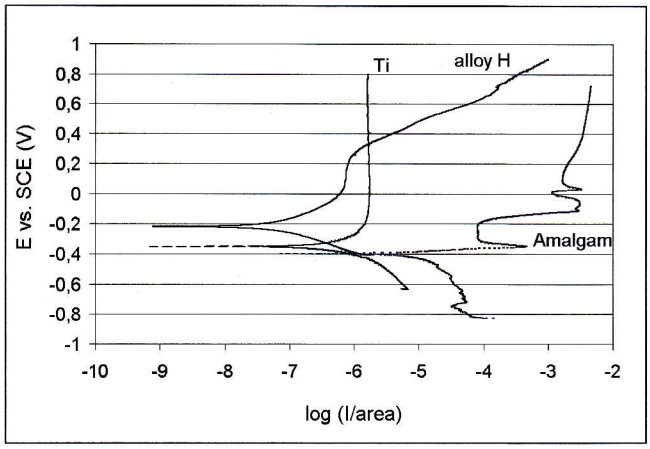

Figure 5. Potentiodynamic curves of Ti, Co-Cr alloy H and dental amalgam.

Figura 5. Curve potenziodinamiche di Ti, lega H al Co-Cr e amalgama dentale.

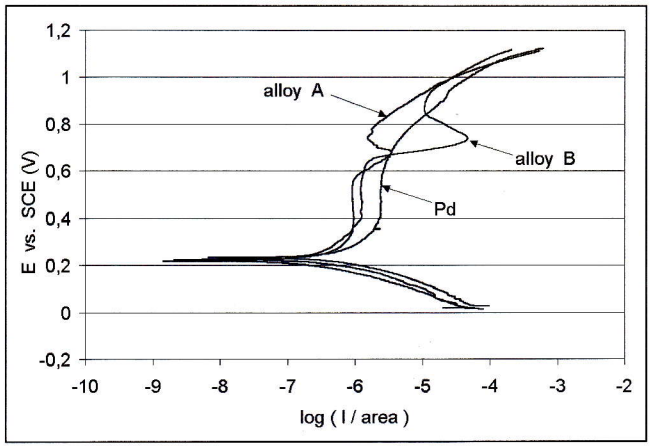

Figure 7. Potentiodynamic curves of the two high Pd content alloys (A and B) and of Pd (99.95 % purity).

Figura 7. Curve potenziodinamiche delle due leghe ad alto titolo di palladio (A e B) e del Pd (purezza 99.95 %).

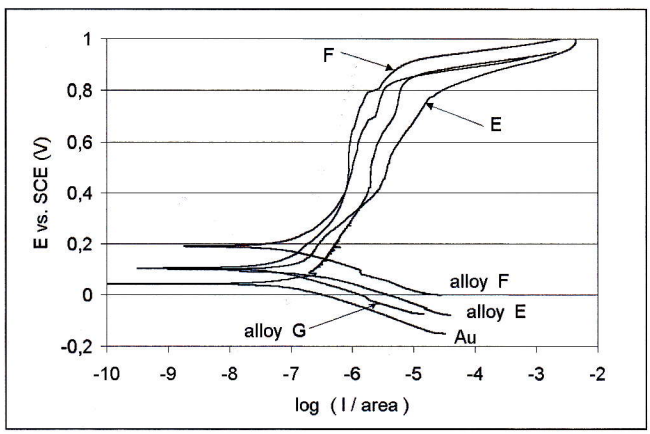

Figure 6. Potentiodynamic curves of alloys E (Au-Pd-Ag), F (Au-Pd), G (high Au content) and Au (99.99% purity).

Figura 6. Curve potenziodinamiche delle leghe E (Au-Pd-Ag), F (Au-Pd), G (alto titolo aureo) e di Au (purezza 99.99%).

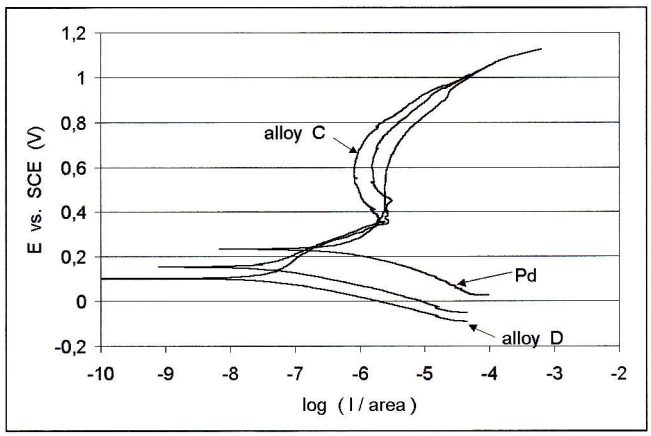

Figure 8. Potentiodynamic curves of the two Pd-Ag alloys (C and D) and of Pd. See that alloy D turned out to be inhomogeneous if observed by backscattered electrons.

Figura 8. Curve potenziodinamiche delle due leghe al Pd-Ag (C e D) e del Pd. La lega D risulta disomogenea all'osservazione mediante elettroni retrodiffusi.

other alloys and pure metals lie between +50 and +250 mV vs SCE. The highest of them are those of Pd, high Pd content alloys (A and B) and Au-Pd alloy (F).

The formation kinetics of passive films in the mentioned materials was studied by E_{corr} recording. The repassivation kinetics is significant for those alloys having surfaces directly exposed to the oral cavity. In this case, wear can reduce or eliminate the passivated layer, enhancing corrosion (7, 14). Pd and high Pd content alloys have the slowest kinetics, taking 2,5 to 5,5 hours to repassivate (Fig.9). Pd takes about twice the time than its own alloys. Furthermore, Ti, alloy H and Pd show an E_{corr} still rising 36 hours after the cathodic polarization (Fig.9). Ag-Pd alloys D and C (Fig. 10) are characterized by an intermediate repassivation kinetics, taking about 50 minutes to repassivate. High Au content alloys (E and G), the Au-Pd alloy (F) and Au (Fig. 10), have a fast repassivation kinetics (less than 15 minutes). Particularly, Au, alloys E and F take less than 6 minutes to repassivate. Ti, alloy H and amalgam (Fig. 11) undertake the most of the repassivation process within 30 minutes. The curve shape (Fig. 9) allows to distinguish the following 3 classes of alloys with respect to the E_{corr} value measured 36 hours after the cathodic reaction. a) low nobility (Ti, alloy H and amalgam), b) mean nobility (Au, Pd, alloys A, B, C, D and E) and c) high nobility (alloys G and F). The E_{corr} values after 36 hours are reported in Table 3. Large differences among the Ecorr values of alloys co-existing in the same oral cavity may enhance galvanic corrosion.

Table 4 reports the results obtained for the polarization resistance R_p, the Tafel slopes (B_{anodic} and $B_{cathodic}$), the OCPs and the corrosion current density values, I_{corr}. The evaluation of I_{corr} has been performed by using a non-linear least-squares fit of the data to the Stern-Geary equation. Results are reported with the associated root mean square values (σ_{n-1}).

Materials can be divided into the following three categories. i) low R_p materials - R_p up to about 100 Kohms, including alloy A, amalgam and Pd; ii) intermediate R_p materials - R_p up to about 250 Kohms, including alloys B, E, F and Ti and iii) high R_p materials - R_p up to 500 KOhms, including Au

Table 3. Galvanic corrosion tests results. $I_{galvanic}$: galvanic corrosion current; E_{couple}: couple voltage; OCP: open circuit voltage stabilized at a variation less than 0.01 mV/s; E_{corr}: corrosion voltage measured after cathodic polarization of the alloy at – 1250 mV vs SCE and after a 36 hours waiting time.

Tab.3. Risultati delle prove di corrosione galvanica. $I_{galvanic}$: corrente di corrosione galvanica; E_{couple}: tensione di coppia; OCP: tensione di circuito aperto stabilizzata ad una variazione inferiore a 0.01 mV/s; E_{corr}: tensione di corrosione dopo polarizzazione catodica della lega a – 1250 mV vs SCE e attesa per 36 ore.

Couple 1st material – 2nd material	Ecouple (mV)	OCP 1st material	OCP 2nd material	E corr 1st material vs. SCE	E corr 2nd material	I galvanic (nA / cm²)
			(mV)			
Au – F	– 215	+ 42	+ 210	+ 112	+ 251	7,0
Ti - B	– 212	– 198	+ 214	– 120	+ 43	17
Ti - amalgam	+ 175	– 198	– 227	– 120	– 220	7
Ti - Pd	– 244	– 198	+ 235	– 120	+ 105	13
Ti – A	– 228	– 198	+ 219	– 120	+ 97.5	11,5
Ti - Au	– 10	– 198	+ 42	– 120	+ 112	11,5
Ti – H	+ 232	– 198	– 297	– 120	– 140	13
Ti – D	– 55	– 198	+ 120	– 120	+ 15	11
Ti – E	– 100	– 198	+ 138	– 120	+ 97.5	11
Ti – C	– 118	– 198	+ 146	– 120	+ 46	14
Ti – G	– 85	– 198	+ 108	– 120	+ 192	16
Ti – F	– 202	– 198	+ 210	– 120	+ 251	14,5
H – G	– 110	– 297	+ 108	– 140	+ 192	6,5
H – C	– 110	– 297	+ 146	– 140	+ 46	5,0
H – F	– 210	– 297	+ 210	– 140	+ 251	12,0
H – D	– 85	– 297	+ 120	– 140	+ 15	5,2
H - Au	– 43	– 297	+ 42	– 140	+ 112	4,5
H – A	– 220	– 297	+ 219	– 140	+ 97.5	11,9
H – B	– 220	– 297	+ 214	– 140	+ 43	9,5
H – E	– 120	– 297	+ 138	– 140	+ 97.5	7,0
H - Pd	– 250	– 297	+ 235	– 140	+ 105	14,5
H - amalgam	+ 190	– 297	– 227	– 140	– 220	– 42,0
G - amalgam	+ 38	+ 108	– 227	+ 192	– 220	– 1700,0
G – A	– 220	+ 108	+ 219	+ 192	+ 97.5	6,7
G – B	– 230	+ 108	+ 214	+ 192	+ 43	6,0
G – E	– 151	+ 108	+ 138	+ 192	+ 97.5	1,5
G – C	– 173	+ 108	+ 146	+ 192	+ 46	4,0
G – D	– 128	+ 108	+ 120	+ 192	+ 15	1,2
G – F	– 216	+ 108	+ 210	+ 192	+ 251	5,6
G – Au	– 120	+ 108	+ 42	+ 192	+ 112	– 1,4
G – Pd	– 248	+ 108	+ 235	+ 192	+ 105	7,0
E – A	– 230	+ 138	+ 219	+ 97.5	+ 97.5	12,5
E – B	– 230	+ 138	+ 214	+ 97.5	+ 43	12,0
E – C	– 153	+ 138	+ 146	+ 97.5	+ 46	5,0
E – D	– 145	+ 138	+ 120	+ 97.5	+ 15	2,9
E – F	– 198	+ 138	+ 210	+ 97.5	+ 251	11,0
E – Au	– 112	+ 138	+ 42	+ 97.5	+ 112	0,1
E – Pd	– 260	+ 138	+ 235	+ 97.5	+ 105	13,0
Amalgam – A	– 17	– 227	+ 219	– 220	+ 97.5	2400,0
Amalgam – B	– 132	– 227	+ 214	– 220	+ 43	1370
Amalgam – E	– 25	– 227	+ 138	– 220	+ 97.5	600
Amalgam – C	– 45	– 227	+ 146	– 220	+ 46	800,0
Amalgam – D	– 23	– 227	+ 120	– 220	+ 15	625,0
Amalgam – F	– 80	– 227	+ 210	– 220	+ 251	1000
Au - Amalgam	+ 102	+ 42	– 227	+ 112	– 220	– 340
Pd - Amalgam	0	+ 235	– 227	+ 105	– 220	– 2500
C – B	– 230	+ 146	+ 214	+ 46	+ 43	5,0
C – D	– 180	+ 146	+ 120	+ 46	+ 15	1,5
C – A	– 230	+ 146	+ 219	+ 46	+ 97.5	5,5
C – F	– 200	+ 146	+ 210	+ 46	+ 251	5,0
C – Au	– 151	+ 146	+ 42	+ 46	+ 112	– 1,2
C – Pd	– 262	+ 146	+ 235	+ 46	+ 105	7,5
D – A	– 248	+ 120	+ 219	+ 15	+ 97.5	7,0
D – B	– 242	+ 120	+ 214	+ 15	+ 43	8,0
D – F	– 227	+ 120	+ 210	+ 15	+ 251	5,8
D – Au	– 128	+ 120	+ 42	+ 15	+ 112	2,0
D – Pd	– 255	+ 120	+ 235	+ 15	+ 105	9,0
A – B	– 250	+ 219	+ 214	+ 97.5	+ 43	3,5
A – F	– 247	+ 219	+ 210	+ 97.5	+ 251	3,5
A – Au	– 235	+ 219	+ 42	+ 97.5	+ 112	– 1,3
A – Pd	– 271	+ 219	+ 235	+ 97.5	+ 105	5,0
B – F	– 248	+ 214	+ 210	+ 43	+ 251	3,5
B – Au	– 222	+ 214	+ 42	+ 43	+ 112	– 2,5
B – Pd	– 270	+ 214	+ 235	+ 43	+ 105	5,0
F – Au	– 204	+ 210	+ 42	+ 251	+ 112	0,3
F – Pd	– 268	+ 210	+ 235	+ 251	+ 105	6,5
Au - Pd	– 264	+ 42	+ 235	+ 112	+ 105	9,5

Material	R_p (KOhms)	I_{corr} (nA / cm²)	I_{crit} (nA / cm²)	OCP (mV) vs.SCE	B_{anod} (V)	B_{catod} (V)
A	87.7 ± 5.1	192.3 ± 22.0	600	219.0 ± 4	0.137 ± 0.04	0.055 ± 0.004
B	121.1 ± 6.7	151.8 ± 34.2	800	214.0 ± 5	0.171 ± 0.06	0.056 ± 0.008
C	330.6 ± 41.2	30.2 ± 1.2	1800	146.0 ± 10	0.069 ± 0.01	0.034 ± 0.002
D	437.7 ± 39.1	28.3 ± 1.3	3280	119.5 ± 7.9	0.127 ± 0.04	0.037 ± 0.003
E	125.4 ± 10.1	68.3 ± 8.1	270	137.8 ± 33.7	0.072 ± 0.02	0.028 ± 0.006
F	205.4 ± 14.9	54.7 ± 13.8	800	210.7 ± 4	0.074 ± 0.02	0.039 ± 0.007
G	324.9 ± 66.5	28.6 ± 9.1	600	108 ± 1.7	0.067 ± 0.01	0.028 ± 0.004
H	493.4 ± 59.1	27.5 ± 4.1	700	- 296.5 ± 4.5	0.073 ± 0.01	0.054 ± 0.004
Amalgam	87.2 ± 9.7	121.2 ± 24.3	480000	- 227.3 ± 3.8	0.060 ± 0.01	0.040 ± 0.004
Pd	102.8 ± 9.9	175.9 ± 16.9	240	234.5 ± 0.5	0.164 ± 0.04	0.056 ± 0.003
Ti	210.7 ± 19.0	116.9 ± 37.6	1600	- 198.0 ± 16	0.138 ± 0.04	0.095 ± 0.024
Au	300.7 ± 46.1	37.2 ± 5.4	300	42.0 ± 6.2	0.117 ± 0.06	0.034 ± 0.007

Table 4. Results of polarization resistance (R_p). Anodic and cathodic Tafel slopes (B_{anod} and B_{cathod}). Open Circuit Potentials at less than 0.01 mV/s variation (OCP). Computed corrosion current values (Stern-Geary equation). Critical passivation currents (I_{crit}) determined from potentiodynamic curves.

Tab.4. Misure di resistenza di polarizzazione (R_p). Tafel slopes anodiche e catodiche (B_{anod} e B_{cathod}). Potenziali di circuito aperto stabilizzati ad una variazione inferiore a 0.01 mV/s (OCP). Valori calcolati (equazione di Stern-Geary) delle correnti di corrosione. Correnti critiche di passivazione (I_{crit}) misurate sulle curve potenziodinamiche.

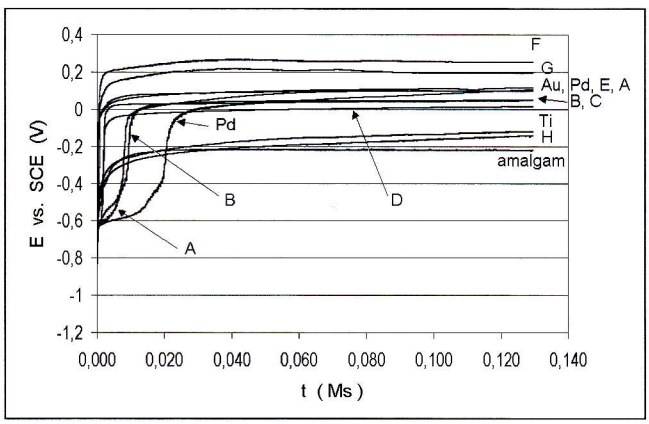

Figure 9. Open circuit potential E_{corr} after cathodic reduction at -1250 mV vs. SCE for 300 s. The high Pd content alloys A and B and pure Pd have the slowest repassivation kinetics.

Figura 9. Andamento degli open circuit potentials (E_{corr}) dopo riduzione catodica a -1250 mV vs.SCE per 300 s. Le leghe ad alto titolo di Pd (A e B) e il Pd hanno le cinetiche di ripassivazione più lente.

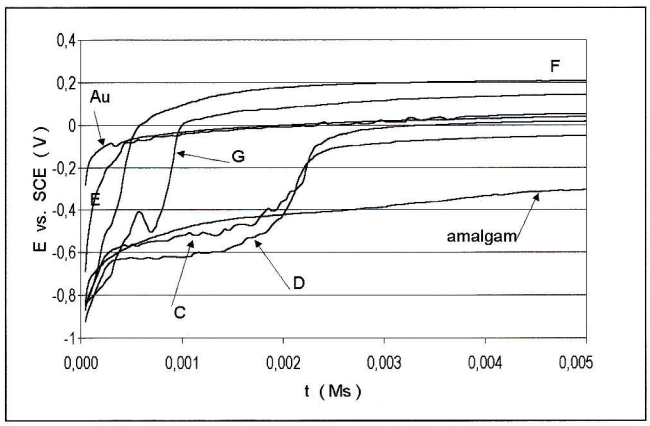

Figure 10. Detail of Figure 9 showing the fast repassivation kinetics of Au, alloy E (Au-Pd-Ag), alloy F (Au-Pd) and alloy G (high Au content alloy). Alloys C and D (Pd-Ag alloys) have intermediate repassivation kinetics.

Figura 10. Dettaglio della figura 9 che mostra le cinetiche di ripassivazione veloci di Au, lega E (Au-Pd-Ag), lega F (Au-Pd) e lega G (ad alto titolo aureo). Le leghe C e D (al Pd-Ag) hanno cinetiche di ripassivazione intermedie.

and alloys C, D, G, and H. On the average, the corrosion currents are inversely proportional to R_p. In any case, I_{corr} values are low and below the range in which patients could feel pain - i.e. 15 to 660 μA/cm² (15). Generally, the lowest Icorr values are found in high Au content alloys, in Au/Pd alloys and in Pd/Ag alloys. However, the last ones show higher passivation currents (I_{crit}) than the previous ones.

Though taking into account the expected extrapolation errors of the Tafel slopes, it turns out that -as absolute values - $B_{anodic} > B_{cathodic}$ for all materials. This means that materials are going to passivate and do not undergo corrosion spontaneously in aerated environment.

The Co-Cr alloy H shows I_{corr} similar to that of the high Au content alloys, in agreement with literature data (16).

The low R_p values of alloy A and amalgam are consistent with microstructural features. In fact, these alloys show inhomogeneous phases and structural constituents that are susceptible to corrosion.

The alloy coupling between Pd and Au/Ag or Pd and Ag leads to materials with mean or high Rp - > 100 or > 250 KOhms respectively - even though the R_p value of pure Pd is low.

3.5. Galvanic corrosion

Table 3 gives the E_{couple} values and the associated galvanic corrosion current $I_{galvanic}$ for all the material couplings. A correlation between the absolute values of the OCP's difference and the galvanic corrosion current of the amalgam/material couplings exists (Fig. 12). The lowest galvanic corrosion currents relate to coupling with Ti and with the Co-Cr alloy H. As far as other amalgam couplings are concerned, no particular dependence of galvanic corrosion current on the alloy chemical composition can be revealed, even though it seems to be favoured by high Pd concentration. The highest galvanic corrosion current values of couplings including the amalgam are again lower than the pain perception threshold. This does not mean that the corrosion products released by the amalgam have no deleterious effects on the tissues around. Such effects have already been discussed (17, 18). Furthermore, dental amalgams release neutral mercury vapours. The release mode depends on the specific amalgam and increases with corrosion (19).

As regards the remaining alloys, the correlation between the above mentioned parameters is rather poor. In these cases, the galvanic corrosion currents are very low (7 ± 4 nA/cm²)

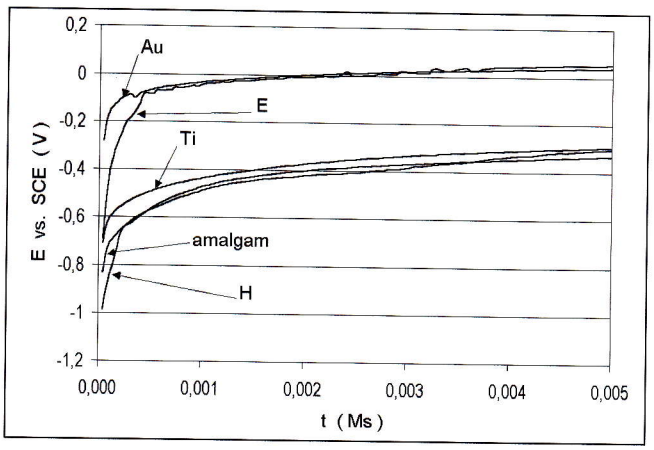

Figure 11. Detail of figure 9 that compares the repassivation kinetics of Ti, Au, amalgam, alloy H (Co-Cr) and alloy E (Au-Pd-Ag).

Figura 11. Dettaglio della figura 9 che mostra il confronto tra le cinetiche di ripassivazione di Ti, Au, amalgama, lega H (al Co-Cr) e lega E (Au-Pd-Ag).

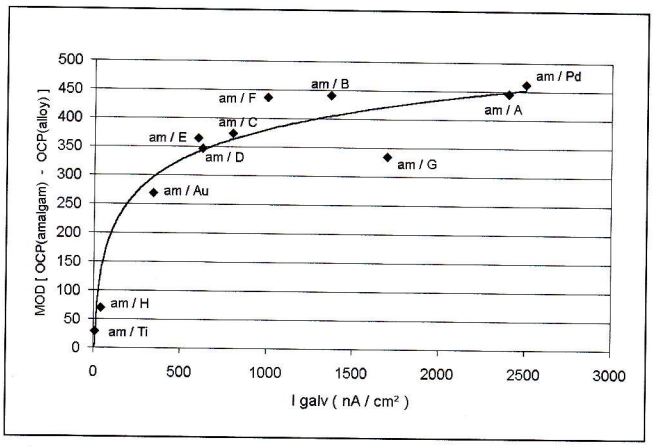

Figure 12. Correlation between the galvanic corrosion current (I_{galv}) and the absolute values of the differences between the open circuit potentials of the couplings with dental amalgam.

Figura 12. Correlazione tra le correnti di corrosione galvanica (I_{galv}) ed il valore assoluto delle differenze tra gli OCP delle coppie con amalgama dentale.

and not perceptible by patients.
The ratio between anodic and cathodic areas is important in galvanic corrosion also. If the anodic surface decreases, the corrosion rate per unit surface increases. Moreover, an electrical contact between different materials can also occur due to the conductive properties of tissue and bones. The resulting electrical circuits are rather complicated, indeed.
When coupling is realized between materials with sufficiently different OCPs - that is $\Delta OCP > 200$ mV - the couple voltage lies between the OCP values of the two materials, as already observed (20,21). In the present work, this condition occurs with couplings including alloy H, Ti and amalgam.
As regards couplings between precious metals alloys, Pd and Au, the anodic and cathodic OCPs are similar. The cathodic reduction reaction rate at the anode and the anodic oxidation reaction rate at the cathode are not negligible. As a consequence, the mixed-potential theory is not applicable for the evaluation of the couple potential (22). In fact the couple potentials fall outside the range defined by the OCPs of the two coupled materials.
Apart from couplings with the amalgam, the $I_{galvanic}$ values are lower than the I_{corr} values computed for single materials (see Table 4).

4. CONCLUSIONS

The corrosion resistance of dental alloys in Ringer artificial saliva depends on both their chemical composition and microstructural homogeneity. The more inhomogeneous alloys show lower polarization resistance and higher corrosion current.
The high Au content alloys have the best properties. However, the combination of Au and Pd or Pd and Ag, provides good corrosion resistance properties.
High Pd content alloys give the highest corrosion current, comparable to that of the dental amalgam, independently on their microstructural homogeneity. The Co-Cr alloy gives a corrosion current similar to that of high Au content alloys. Ti has a good corrosion resistance, better than high Pd content alloys.
All pure metals and alloys subjected to galvanic coupling produce negligible corrosion current density - within 10 nA/cm^2 - . Inversely, couplings with the dental amalgam give galvanic corrosion currents between 340 and 2500 nA/cm^2. The only couplings accepted by the amalgam are with the Co-Cr alloy and Ti. They are characterized by currents lower than 40 nA/cm^2. As a consequence, the amalgam should be used with caution in the oral cavity.
The present work underlines the role of galvanic corrosion in the oral cavity, especially when significant difference between anodic and cathodic areas exists.
Pd, high Pd content alloys and Pd-Ag alloys have the slowest passivation kinetics. Hence, the application of these materials under wear conditions should be carefully evaluated.
Further tests with artificial saliva less aggressive than the Ringer one and the use of de-aerated solutions would allow going deeper into the present study.

REFERENCES

1) R. G. Craig (Ed.). Restorative dental materials. Ninth. Ed. St. Luis: Mosby. (1993)
2) P. Menghini, P. Battaini. Metallurgia in odontoiatria. Milano: Masson. (1997).
3) S. Canay, N. Hersek, A. Çulha, S. Bilgiç. Evaluation of titanium in oral conditions and its electrochemical corrosion behaviour. J. Of oral Rehab. 25 : 759 – 764. (1998).
4) T. Albrektsson, L. Sennerby. State of the art in oral implants. J.Clin. Periodontol. 18: 474 - 481. (1991)
5) R. Adell, B. Eriksson, U. Lekholm, P. I. Brånemark, T. Jemt. Studio con lungo follow-up su impianti osteointegrati per la ricostruzione delle mascelle completamente edentule. Quintessence International. 3 : 235 - 247. (1992).
6) L. Reclaru, J. M. Meyer. Study of corrosion between a titanium implant and dental alloys. J. Dent. 22 : 159-168. (1994).
7) K. Elagli, M. Traisnel, H. F. Hildebrand. Electrochemical behaviour of titanium and dental alloys in artificial saliva. Electrochimica Acta. Vol. 38, N° 13, 1769-1774. (1993).
8) E. J. Sutow, D. W. Jones, G. C. Hall. Correlation of dental amalgam crevice corrosion with clinical ratings. J. Dent. Res. 68 (2). 82 – 88. (february 1989).
9) L. Reclaru, J. M. Meyer. Effects of fluorides on titanium and other dental alloys in dentistry. Biomaterials. 19 : 85 – 92. (1998).
10) J. D. Bumgardner, Berit I Johansson. Effects of tita-

nium-dental restorative alloy galvanic couples on cultured cells - J. Biomed.Mater. Res. (Appl. Biomater.) 43: 184-191. (1998).
11) R. Baboian. Corrosion tests and standards. ASTM manual series : MNL20. Philadelphia. (1995).
12) C. Mülders, M. Darwish, R. Holze. The influence of alloy composition and casting procedure upon the corrosion behaviour of dental alloys: an in vitro study. J.of Oral Rehab. 23: 825 – 831. (1996).
13) E. Angelini, P. Piccardo, M. R. Pinasco, F. Rosalbino. Relazione tra microstruttura e resistenza alla corrosione e al tarnish di leghe auree utilizzate in odontoiatria protesica. La Metallurgia Italiana. 6: 25 – 31. (1998).
14) R. A. Buchanan, E. D. Rigney, J. M. Williams. Ion implantation of surgical Ti-6Al-4V for improved resistance to wear-accelerated corrosion. J.Biomed.Materials Res. 21 : 335 – 336. (1987).
15) G. Ravnholt. Corrosion current and pH rise around titanium coupled to dental alloys. Scand. J. Dent. Res. 96: 466 – 472. (1988).
16) P. R. Mezger, M. M. A. Vrijhoef, S. M. Newman, E. H. Greener. The corrosion resistance of a new cobalt-chromium-molibdenum-ceramic alloy. J.of Oral Rehab., 15: 421 – 428. (1988).
17) J. D. Bumgardner, Berit I Johansson. Galvanic corrosion and cytotoxic effects of amalgam and gallium alloys coupled to titanium. Eur J. Oral Sci. 104: 300-308. (1996)
18) H. F. Hildebrand, J. C. Hornez, N. Späth. Biological and clinical effects of alloys used for dental restorations. Third European Precious Metals Conference, Florence 17 – 19 september 1997.
19) R. I. Holland. Use of potentiodynamic polarization technique for corrosion testing of dental alloys. Scand. J. Dent. Res. 19: 75-85. (1991).
20) R. Venugopalan, L. C. Lucas. Evaluation of restorative and implant alloys galvanically coupled to titanium. Dent. Mater. 14 : 165 – 172 (June 1998).
21) B. Grosgogeat, L. Reclaru, M. Lissac, F. Dalard. Measurement and evaluation of galvanic corrosion between titanium/Ti6Al4V implants and dental alloys by electrochemical techniques and auger spectrometry. Biomaterials. 20: 933 – 941. (1999).
22) J. R. Scully. In: " Electrochemical Methods for laboratory corrosion testing ". ASTM STP 1000, Philadelphia. 351 – 378 (1989).

ABSTRACT

COMPORTAMENTO A CORROSIONE ELETTROCHIMICA DI LEGHE E METALLI PER IMPIEGHI DENTALI IN SALIVA ARTIFICIALE

Nell'ambito delle riabilitazioni protesiche odontoiatriche esiste un'ampia diversificazione di soluzioni. È frequente che nella stessa cavità orale coesistano combinazioni di materiali metallici, quali amalgami, leghe di metalli preziosi, titanio, leghe al cobalto-cromo, ecc. I vari fluidi corporei presenti in questo ambiente possono favorire la corrosione dei singoli materiali, oltre che la corrosione galvanica tra le diverse coppie. Lo studio di questi processi in vitro è molto complesso, poiché la loro intensità dipende da un gran numero di parametri quali il pH, la composizione e conducibilità del mezzo elettrolitico, la sua aerazione o deaerazione, il potenziale degli elettrodi e il rapporto tra le aree di anodo e catodo. La superficie dei materiali esposta ai fluidi della cavità orale è in contatto con l'ossigeno. Vi sono superfici metalliche libere nel caso di resaturi in amalgama, scheletrati in Ti, restauri in lega-ceramica o lega-resina. Lo scopo del presente lavoro è caratterizzare mediante tecniche elettrochimiche la corrosione di leghe dentali, amalgami e metalli commercialmente puri (Tab.1) in saliva artificiale del tipo Ringer, in presenza di ossigeno.

Le misure elettrochimiche sono state condotte con una cella a 3 elettrodi, mediante un potenziostato/galvanostato del tipo EG&G PAR modello 273A. La Tab.2 riassume le condizioni di prova. La corrosione galvanica tra le coppie di materiali analizzate è stata valutata utilizzando una cella con due elettrodi di lavoro, opportunamente collegata allo stesso potenziostato. I materiali sono stati preventivamente esaminati al microscopio elettronico a scansione utilizzando il segnale ad elettroni retrodiffusi, per valutare le disomogeneità microstrutturali (Fig. 1, 2, 3, 4). Escludendo i metalli puri e due leghe (C e G - Tab.1), si osservano disomogeneità microstrutturali che possono favorire fenomeni di corrosione. Le prove di corrosione potenziodinamiche mostrano un buon comportamento per tutti i materiali, ad esclusione dell'amalgama dentale (Fig. 5, 6, 7, 8). Le leghe ad alto titolo di Pd hanno comunque una resistenza alla corrosione inferiore. Il comportamento migliore è dato dalle leghe ad alto titolo aureo, dalle leghe Au-Pd e dalle leghe Pd-Ag, come è riassunto dalla Tab. 4. I risultati delle misure di corrosione galvanica sono riportati in Tab. 3. Le correnti di corrosione galvanica ($I_{galvanic}$) tra le varie coppie risultano solitamente inferiori alle correnti di corrosione dei singoli materiali (I_{corr} – Tab. 4), e non superano i 15 nA/cm^2. Fanno eccezione gli abbinamenti con l'amalgama dentale che presentano correnti comprese tra 340 e 2500 nA/cm^2 (Tab. 3, Fig. 12). Le cinetiche di ripassivazione dei vari materiali sono state studiate dopo polarizzazione catodica (Fig. 9, 10, 11). Le leghe ad alto titolo di Pd, le leghe Pd-Ag ed il Pd hanno le cinetiche più lente e non dovrebbero essere utilizzate in presenza di usura.

I risultati ottenuti dimostrano che la resistenza a corrosione delle leghe dentali in saliva artificiale Ringer dipende sia dalla loro composizione chimica che dal grado di omogeneità microstrutturale. Le leghe ad alto titolo di Pd, indipendentemente dalla loro omogeneità microstrutturale, danno i valori più alti di corrente di corrosione, paragonabili a quella dell'amalgama dentale. La lega Co-Cr ha una corrente di corrosione simile a quelle delle leghe ad alto titolo aureo. Il Ti ha una buona resistenza a corrosione, migliore delle leghe ad alto titolo di Pd.

Il lavoro svolto mette in rilievo il ruolo della corrosione galvanica in cavità orale, che può essere importante quando vi sia una significativa differenza tra le aree anodiche e catodiche. L'uso dell'amalgama dentale dovrebbe essere evitato, viste le elevate correnti di corrosione galvanica ad essa associate. L'impiego di salive artificiali meno aggressive della Ringer e l'uso di soluzioni deaerate consentirebbe un approfondimento del presente studio.